COMMUNICATION

Hydrogels toughened by biominerals providing energy-dissipative sacrificial bonds

Received 00th January 20xx,
Accepted 00th January 20xx

DOI: 10.1039/x0xx00000x

Kazuki Fukao,[a] Kazuki Tanaka,[a] Ryuji Kiyama,[a] Takayuki Nonoyama★[b,c] and Jian Ping Gong★[b,c,d]

Inspired by bone tissues, we mineralized low crystalline hydroxyapatite (HAp) particles in double network (DN) hydrogels, and we observed that the HAp minerals toughens the gels. The contribution of dissipated energy from HAp minerals was over 500 % higher than that from polymer in tensile deformation. We elucidated that the amorphous parts in the HAp minerals break at deformation, acting as energy-dissipative sacrifical bonds. This result implies that not only brittle polymer network but also mineral can work as sacrificial bond to toughen soft materials.

Over the past two decades, great progress has been made in the synthesis of hydrogel materials with high strength and toughness, which significantly broadens the potential application of the material, especially as soft and wet structural materials for bio-applications. Two strategies, "network uniformalization" and "energy dissipative sacrificial bonds" are mainly adopted to improve the mechanical properties of hydrogels. For example, Slide-ring gels and Tetra-PEG gels show high strength and extensibility by improving the network inhomogeneity.[1,2] Double network (DN) gels show high fracture toughness by sacrificial fracture of the brittle network and weak physical bonds.[3–8] It has been clarified that by incorporating reversible/irreversible sacrificial bonds/structure that preferentially break under deformation, global fracture of a hydrogel can be prevented and the material becomes tough and strong. The DN gel consists of two interpenetrated polymer networks with contrasting mechanical properties.[4,6,9,10] The first network, made of fully pre-stretched, densely crosslinked polyelectrolyte, is rigid and brittle, and the second network, made of loosely cross-linked neutral polymer, is soft and stretchable. During the deformation of a DN gel, the first brittle network is preferentially fractured in large areas because the second soft network, entangled within the first network, transfers the stress from initial fracture point or stress concentration point to the surrounding network. The preferential fracture of the first network in large areas dissipates a huge amount of energy, resulting in the high toughness of the DN gel. The high toughness is almost comparable to that of natural rubber and articular cartilage tissue. Here, the sacrificial bond principle demands a brittle and stiff first network that fractures preferentially before the second network.

Ceramics and minerals are representative materials possessing a brittle and stiff nature. Among them, the calcium phosphate salt, hydroxyapatite (HAp) is a promising biomineral. HAp is the main inorganic component of bones and teeth to give them enough stiffness and strength for supporting their body. Besides, HAp can be synthesized in aqueous and mild condition that is capable of making composite with hydrogel materials.[11] It is known that HAp easily forms defects in its lattice and becomes brittle due to easy exchange from constitutive ions to others.[12,13] It has been suggested that the fracture of microscopic poly-crystals would be one of the energy dissipative mechanisms to prevent fatal bone fracture in bone.[14] Also, HAp possesses osteoconductivity to induce bone formation. HAp coated hydrogels can strongly bond to bone tissues because they induce ingrowth of bone into the permeable gel matrix.[15–17]

In this study, we broaden the current sacrificial bond principle of "synthetic polymers" to bioceramics, by incorporating HAp poly-crystals as "sacrificial bonds" into a double network gel consisting of two identical neutral polymers. We show that the double network gel from neutral polymers alone is weak while incorporation of HAp as sacrificial bonds significantly toughens the gel. **Fig. 1a** shows a schematic illustration of the HAp-polymer double network (HAp/DN) hydrogel. First, a neutral polymer gel is prepared. The neutral polymer gel, serving as a substrate for HAp crystallization, is

[a] *Graduate School of Life Science, Hokkaido University, Sapporo, 001-0021, Japan*
[b] *Faculty of Advanced Life Science, Hokkaido University, Sapporo, 001-0021, Japan. E-mail: nonoyama@sci.hokudai.ac.jp, gong@sci.hokudai.ac.jp*
[c] *Global Station for Soft Matter, Global Institution for Collaborative Research and Education (GI-CoRE), Hokkaido University, Sapporo, 001-0021, Japan*
[d] *Institute for Chemical Reaction Design and Discovery (WPI-ICReDD), Hokkaido University, Sapporo, 001-0021, Japan*

† Electronic Supplementary Information (ESI) available: [details of any supplementary information available should be included here]. See DOI: 10.1039/x0xx00000x

chosen because it is osmotically inert against ionic solution and maintains the same volume in the precursor solutions for HAp crystallization. To obtain the gel incorporating HAp, namely as HAp single network (HAp/SN), the gel is repeatedly soaked in calcium chloride solution and dipotassium phosphate solution alternatingly. During the alternating immersion, these ions diffuse into the gel matrix and form submicron scale HAp poly-crystals. Because this HAp poly-crystal is much larger than the network mesh size, the HAp is physically interlocked within the network. As a result, the HAp/SN gel is expected to be rigid and brittle, in comparison to the first SN gel. After that, the second soft and stretchable network is polymerized in the presence of HAp-crystallized gel. This second network is topologically entangled with the brittle HAp crystallized network. The soft materials are toughened by the bioceramics which act as sacrificial bonds thereby broadening the sacrificial bond principle beyond synthetic polymeric materials category.

In particular, we employed poly(dimethylacrylamide) (PDMAAm) both as the first and second networks. The first PDMAAm gel was synthesized at room temperature by radical polymerization from an aqueous solution containing 1 M DMAAm as a monomer, 2 mol% MBAA as a cross-linker, and 0.1 mol% KPS and 1.0×10^{-4} vol% TEMED as initiators. Then HAp mineralization was carried out in the first PDMAAm gel by alternatingly immersing the gel in two solutions, one containing 300 mM dipotassium phosphate and the other 500 mM calcium chloride.[17,18] This alternative soaking process was repeated for n cycles (n = 0, 1, 3, 5 and 7). After the alternating soaking, the mineralized PDMAAm gel was immersed in $CaCl_2$ aqueous solution at 35 °C over 1 day to ripen the amorphous calcium phosphate (ACP) to HAp (HAp/SN gel) (see details in Supplementary Information). The HAp/SN gel became hard and brittle compared to the PDMAAm SN gel (**Fig. 2a**). After that, this brittle HAp/SN gel was immersed in a second DMAAm solution containing 2 M DMAAm, 0.2 mol% MBAA, and 0.1 mol% KPS, and thermal polymerization was performed again at 60 °C in air atmosphere to obtain the HAp/DN gel.

Fig. 1b shows images of HAp/DN gels at different mineralization cycle numbers, n. All the gels were cut to the same size. The transparent gel gradually became opaque with increasing n, showing no distinct volume change. The cross-sectional morphology of the mineralized HAp in the solidified gel specimen was observed by transmission electron microscopy

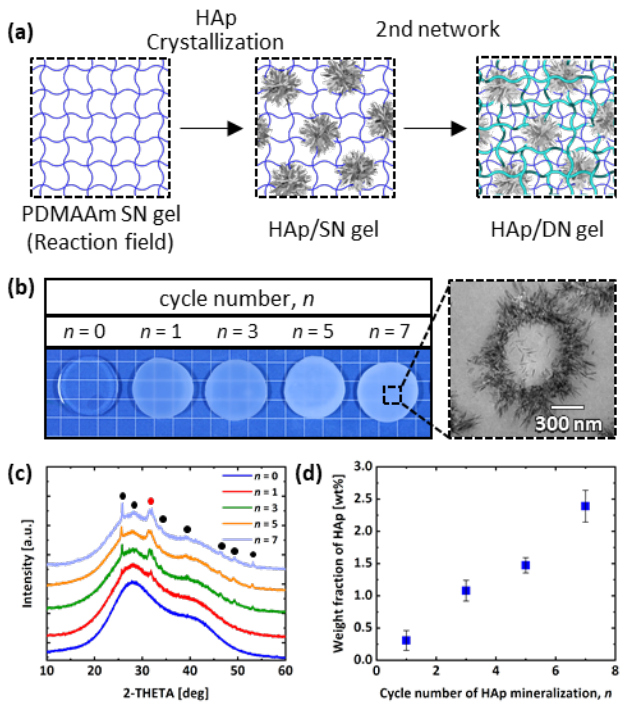

Fig. 1 (a) Schematic illustrations of HAp/DN gel concept. The first gel is a reaction field of HAp mineralization. The first network gel becomes brittle after the mineralization. Then, the soft second network is polymerized in the presence of HAp brittle network. (b) Appearances of HAp/DN gels in different cycle number of HAp mineralization n, and TEM image of HAp poly-crystal mineralized in the gel (n = 7). (c) XRD profiles of wet-state HAp/DN gels. Dots show the HAp peaks. (d) Weight fraction of HAp in HAp/DN gels for different n.

(TEM). Hollow and spiny spherical HAp clusters with ~800-nm diameter were observed. The cluster is composed of the acicular monocrystals with ~100-nm length in the long axis (c-axis). This polycrystalline sphere was much larger than network size of the PDMAAm gel (~10 nm), meaning that the polymer network is incorporated within the HAp cluster. The X-ray diffraction (XRD) profiles of wet-state HAp-DN gels show relatively sharp peaks and broad shoulders, which can be assigned to the characteristic peaks of the HAp crystals and amorphous water background, respectively (**Fig. 1c**). The HAp peaks became obvious with increasing n. The red-dotted peaks of around 32 degrees of 2θ hardly split, indicating that the mineralized HAp has low crystallinity. The weight fraction of HAp in the gel linearly increased with increasing n, reaching the maximum fraction of around 2.4 wt% at n=7 (**Fig.1d**). The mineral

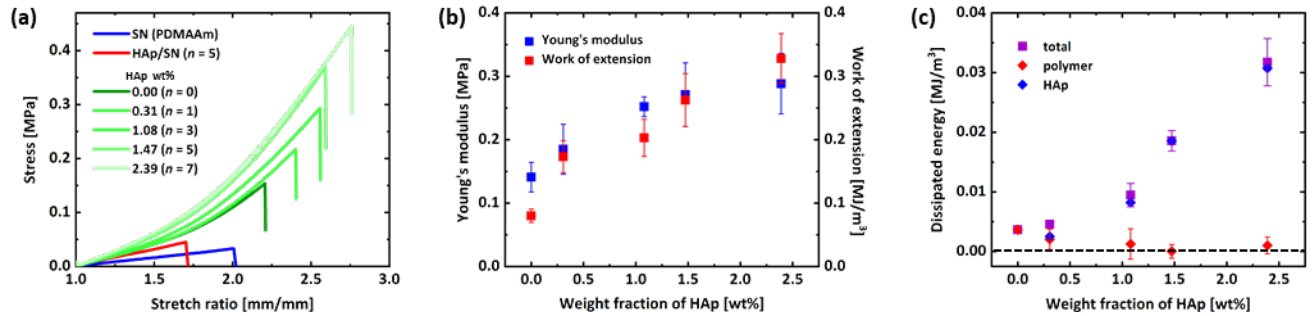

Fig. 2 Tensile mechanical properties of HAp/DN gels with different weight fractions of HAp. (a) Stress-Stretch ratio curves of SN (blue), HAp/SN (red) and HAp/DN (green) gels. (b) Young's modulus (blue) and work of extension (red) as a function of HAp weight fraction. (c) Dissipated energies of total (purple), HAp (blue) and polymer (red). The dissipated energies were estimated from the mechanical hysteresis of cyclic test for samples stretched up to λ=2.

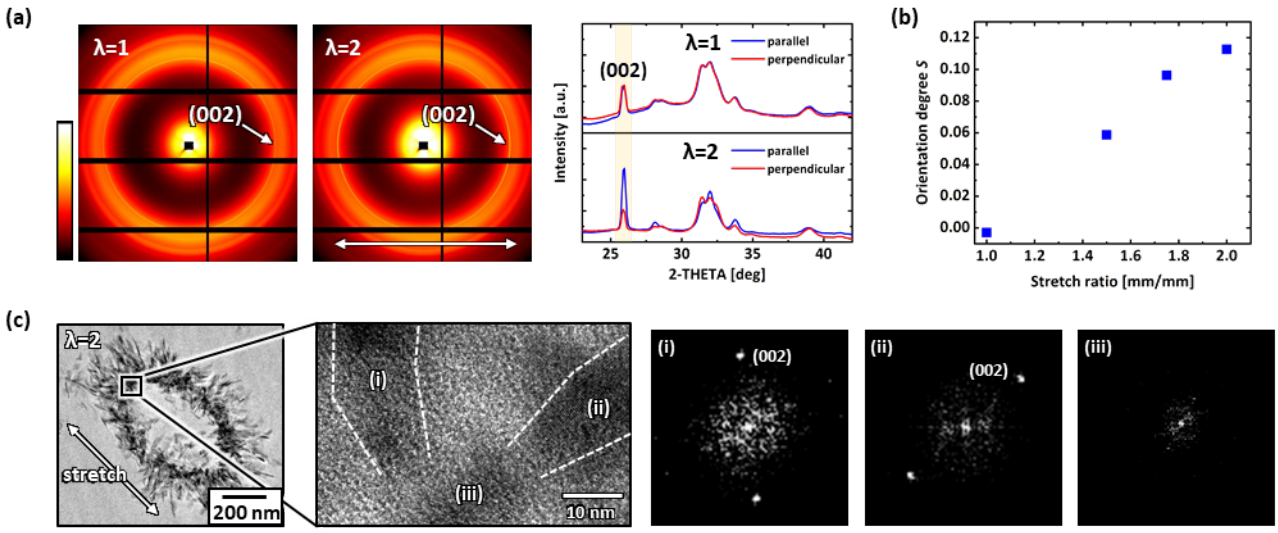

Fig.3 Microscopic anisotropy of HAp under macroscopic deformation of the HAp/DN hydrogel (n=5). (a) Synchrotron WAXD diffraction patterns, and 1D profiles isolated into parallel (blue) and perpendicular (red) against the stretch direction; non stretched sample (λ=1) and stretched sample (λ=2). The stretch directions are defined on horizontal axis. (b) Orientation degrees, S, of HAp (002) plane as a function of stretch ratio. (c) TEM images of HAp poly-nanocrystal at stretched state (λ=2). Lattice image around interconnecting spiny HAp monocrystals. TEM image and selected-area 2DFFT profiles show that HAp polycrystalline sphere consists of not only spiny monocrystals, (i) and (ii), but also amorphous calcium phosphate connecting monocrystals, (iii).

formation was concentrated on the surface of the gel above n=7 to form micro-cracks on the surface.

Fig.2 shows the uniaxial tensile profiles of HAp-DN gels. With increasing the weight fraction of HAp, the Young's modulus, the maximum strength and stretch ratio, and the work of extension (the area below the stress-stretch ratio curves) to sample fracture obviously increases even though the HAp weight fractions were very low (**Fig. 2a-b**). Moreover, the total energy dissipation E_{Total} during the loading to a stretch ratio λ=2, which is estimated from the hysteresis area enclosed by the loading and unloading curves, increased with increasing in HAp fraction, meaning that sacrificial bonds worked to dissipate energy (**Fig S1**). Three possible mechanisms contributing to E_{Total} should be considered; polymer chain rupture energy (E_P), HAp rupture energy (E_{HAp}) and debonding energy between polymer and HAp surface ($E_{P\cdot HAp}$). Since the adsorption of polymer to HAp is a physical interaction, the contribution from debonding energy $E_{P\cdot HAp}$ is reversible. To clarify the reversibility of energy dissipation, we carried out two cycles of load-unload deformations with different waiting times between the two cycles. If the energy dissipation contains recoverable components, the 2nd loading curve should appear above the unloading curve of 1st loading. In both waiting times, 0 and 30 min, the second loading curve of HAp-DN gel overlapped with the unloading curve of the first loading. This result shows that the energy dissipation is irreversible, and the contribution of $E_{P\cdot HAp}$ is almost zero (**Fig. S2**). To estimate E_P, we used a method described in Supplementary Information (**Fig. S3**). Briefly, we compared two samples that were non-stretched HAp/DN gel and pre-stretched HAp/DN gel (λ=2). Both samples were immersed in HCl solution (3.5 wt%) for 1 min to dissolve HAp mineral. No detectable polymer decomposition was induced by the acid treatment (**Fig. S4**). Then, the two samples without HAp were stretched to λ=2, and their stress- stretch ratio curves were compared. E_P was estimated from the difference of their work of extension. **Fig.2c** showed that the contribution of polymer network rupture in dissipated energy was quite small and almost constant in any HAp fractions. On the other hand, the contribution of HAp rupture greatly increased with increasing HAp weight fraction and reached 30-fold that of polymer at most. These results show that even a small amount of HAp can provide sacrificial bonds and enhance toughness of soft polymeric gel matrix.

The major energy dissipation of HAp/DN gel was due to HAp. To evaluate how HAp dissipates energy, synchrotron wide angle X-ray diffraction (WAXD) and TEM observation of the HAp/DN gel at stretch ratios from λ=1 to 2 were performed for samples with n=5. **Fig.3a** shows 2D diffraction patterns and 1D profiles in parallel and perpendicular directions with respect to the stretching axis that is the horizontal direction in the 2D image. At λ=1, isotropic Debye-Scherrer rings assigned to HAp were observed, and the corresponding 1D profiles of parallel and perpendicular directions also overlapped. The HAp polycrystals were completely isotropic before the stretching of the sample. At λ=2, the isotropic rings changed to crescent arcs, and the diffraction peaks became anisotropic. Especially the (002) plane of HAp at 26° of 2θ, being perpendicular to c-axis, was highly orientated. In addition, the deconvolution of the dense peak around 32° revealed that the c-axis was oriented to the stretch direction (**Fig. S5**). This orientation of (002) plane was quantitatively evaluated by Herrmann's orientation function, S.[19,20] The S=0 and 1 mean that the HAp (002) plane is perfectly random and perpendicular to stretching direction, respectively. The S linearly increased with increasing the stretch ratio (**Fig.3b**), identifying that the c-axis of HAp aligns into parallel to the stretch direction. To reveal, in more detail, the HAp structure before and after deformation, TEM observation of HAp morphology at λ= 2 was carried out (**Fig.3c**). The spiny spheres were deformed to oval spheres along the stretching direction, while the acicular monocrystals show less fracture. The higher

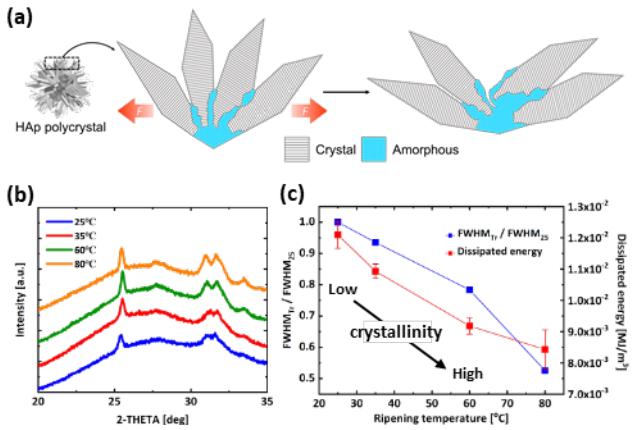

Fig. 4 Dependence of crystallinity of HAp on toughness of HAp/DN hydrogel. (a) Expected mechanism of energy dissipation. The amorphous phase is preferentially deformed and fractured under stretching because HAp crystals are too rigid to be deformed. (b) X-ray diffraction profiles of HAp/DN (n=5) prepared by different ripening temperatures. (c) Ratio of FWHM of the (002) peak at 26° for samples ripened at various temperatures in relative to that ripened at 25°C (left axis) and dissipated energy (right axis) as a function of ripening temperature.

magnification observation revealed that an amorphous calcium phosphate phase existed and interconnected the ends of the acicular HAp monocrystal.

From these facts, a probable energy dissipative mechanism of mineralized HAp is illustrated in **Fig.4a**. The HAp mineralized in aqueous media at mild temperature contains much amorphous phase, and the stiffness of the HAp crystal is much higher than that of amorphous calcium phosphate. When tension is applied to the sphere via the polymer network, the weak and brittle amorphous phase is preferentially ruptured to allow the long axis (c-axis) of spiny HAp monocrystals align into the stretching direction. Therefore, the main energy dissipation would be due to the rupture of the amorphous phase of mineralized HAp. To reveal that, the effect of crystallinity of HAp on dissipated energy was evaluated. The crystallinity was controlled by the ripening temperature, T_r, of HAp crystallization. **Fig.4b** shows XRD profiles of HAp/DN gels with different T_r. The characteristic peaks became sharp at elevated T_r. The degree of crystallinity was evaluated from the ratio of full widths at half maximum (FWHM) of (002) peak for each T_r relative to that of 25 °C, where small value of FWHM ratio shows high crystallinity (**Fig. 4c**). The dissipated energy of uniaxial deformation was inversely proportional to the crystallinity, so that this result reveals that the main energy dissipation of HAp/DN gel is within the amorphous phase of HAp, and the spiny HAps work as transmitters of tension to the interconnected amorphous phase. This indicates that the HAp monocrystals are too stiff to serve as sacrificial bonds.

In summary, a biomineral can provide sacrificial bonds to toughen a polymeric matrix in the same way as conventional brittle polymer networks and weak physical bonds. During macroscopic deformation of the polymeric matrix, stress is transferred from the polymer network to the brittle biomineral incorporated in the polymer network. HAp crystal is too strong to be ruptured, while the amorphous HAp phase can be deformed and ruptured to gain energy dissipation. The low crystalline biomineral has advantage on toughening the matrix. Therefore, this may be one of the reasons why bone tissues contain much amorphous phase of biomineral. This toughening strategy expands the universality of the sacrificial bond principle beyond polymer systems and broadens the options to design tough and functional materials.

Conflicts of interest

There are no conflicts to declare.

Acknowledgements

This research was financially supported by JSPS KAKENHI Grant numbers JP17H06144, 17H06376. This research was also partially funded by ImPACT Program of Council for Science, Technology and Innovation (Cabinet Office, Government of Japan). Institute for Chemical Reaction Design and Discovery (ICReDD) was established by World Premier International Research Initiative (WPI), MEXT, Japan. We thank the open facility of Hokkaido University Sousei Hall, for using FE-TEM.

Notes and references

1 Y. Okumura and K. Ito, *Adv. Mater.*, 2001, **13**, 485–487.
2 T. Sakai, T. Matsunaga, Y. Yamamoto, C. Ito, R. Yoshida, S. Suzuki, N. Sasaki, M. Shibayama and U. Il Chung, *Macromolecules*, 2008, **41**, 5379–5384.
3 J. P. Gong, Y. Katsuyama, T. Kurokawa and Y. Osada, *Adv. Mater.*, 2003, **15**, 1155–1158.
4 R. E. Webber, C. Creton, H. R. Brown and J. P. Gong, *Macromolecules*, 2007, **40**, 2919–2927.
5 J. P. Gong, *Soft Matter*, 2010, **6**, 2583–2590.
6 T. Nakajima, T. Kurokawa, S. Ahmed, W. L. Wu and J. P. Gong, *Soft Matter*, 2013, **9**, 1955–1966.
7 T. L. Sun, T. Kurokawa, S. Kuroda, A. Bin Ihsan, T. Akasaki, K. Sato, M. A. Haque, T. Nakajima and J. P. Gong, *Nat. Mater.*, 2013, **12**, 932–937.
8 F. Luo, T. L. Sun, T. Nakajima, T. Kurokawa, Y. Zhao, K. Sato, A. Bin Ihsan, X. Li, H. Guo and J. P. Gong, *Adv. Mater.*, 2015, **27**, 2722–2727.
9 Y. H. Na, T. Kurokawa, Y. Katsuyama, H. Tsukeshiba, J. P. Gong, Y. Osada, S. Okabe, T. Karino and M. Shibayama, *Macromolecules*, 2004, **37**, 5370–5374.
10 S. Ahmed, T. Nakajima, T. Kurokawa, M. Anamul Haque and J. P. Gong, *Polymer (Guildf).*, 2014, **55**, 914–923.
11 N. Rauner, M. Meuris, M. Zoric, J. C. Tiller, Nature, 2017, **543**, 407-410.
12 L. Rintoul, E. Wentrup-Byrne, S. Suzuki and L. Grøndahl, *J. Mater. Sci. Mater. Med.*, 2007, **18**, 1701–1709.
13 J. F. Cawthray, A. L. Creagh, C. A. Haynes and C. Orvig, *Inorg. Chem.*, 2015, **54**, 1440–1445.
14 U. G. K. Wegst, H. Bai, E. Saiz, A. P. Tomsia and R. O. Ritchie, *Nat. Mater.*, 2015, **14**, 23–36.
15 T. Nonoyama, S. Wada, R. Kiyama, N. Kitamura, M. T. I. Mredha, X. Zhang, T. Kurokawa, T. Nakajima, Y. Takagi, K. Yasuda and J. P. Gong, *Adv. Mater.*, 2016, **28**, 6740–6745.
16 S. Wada, N. Kitamura, T. Nonoyama, R. Kiyama, T. Kurokawa, J. P. Gong and K. Yasuda, *Acta Biomater.*, 2016, **44**, 125–134.
17 R. Kiyama, T. Nonoyama, S. Wada, S. Semba, N. Kitamura, T. Nakajima, T. Kurokawa, K. Yasuda, S. Tanaka and J. P. Gong, *Acta Biomater.*, 2018, **81**, 60–69.

18 J. C. Góes, S. D. Figueiró, A. M. Oliveira, A. A. M. Macedo, C. C. Silva, N. M. P. S. Ricardo and A. S. B. Sombra, *Acta Biomater.*, 2007, **3**, 773–778.
19 S. Mann, B. R. Heywood, S. Rajam and J. D. Birchall, *Nature*, 1988, **334**, 692–695.
20 K. Fukao, T. Nonoyama, R. Kiyama, K. Furusawa, T. Kurokawa, T. Nakajima and J. P. Gong, *ACS Nano*, 2017, **11**, 12103–12110.